

Evaluation of Liquefaction Based On Shear Wave Velocity Using Machine Learning

Shaymaa Kennedy¹, Maher Alabbod², Iman M. Jaafar³

^{1,3} Basrah University, Basrah, Iraq.

² West Virginia University, U.S.A.

Corresponding author: Shaymaa.kennedy@uobasrah.edu.iq

Abstract - Liquefaction investigations use a variety of approaches based on field and laboratory tests. The paper describes a study designed to determine the probability of soil liquefaction in a region covering Turkey and Iraq. We used machine learning approaches, particularly Random Forest (RF) models, to build and test models to estimate the chance of liquefaction, with shear wave velocity playing a critical role. In addition, earthquake magnitude and peak acceleration were considered important variables. The dataset includes soil attributes such as effective vertical stress ($\sigma'v0$), soil type, shear wave velocity (V_s), and earthquake parameters including peak horizontal acceleration (PGA) and magnitude (M), allowing for the computation of liquefaction risk as actual values. The results indicate that Random Forest predicted soil liquefaction potential with a remarkable 92.5% accuracy using only 20% of the dataset. This study adds to the progress of risk assessment approaches in earthquake-prone locations, hence improving infrastructure resilience and catastrophe protection.

Keywords: Liquefaction, shear wave velocity, Random Forest, Probability of liquefaction.

1. Introduction

The estimation of soil liquefaction potential is a crucial element in geotechnical engineering, particularly in seismically active areas. Liquefaction, the process by which saturated soil loses strength and stiffness due to increasing pore water pressure during earthquakes, can cause significant structural damage and fatalities. Various approaches for assessing liquefaction potential have been developed, including those based on shear wave velocity (V_s), a fundamental feature that reflects soil stiffness and strength.

Numerous investigators have provided various approaches for evaluating liquefaction based on in-situ measurements such as shear wave velocity. [9], [14], [15] [11]. In 1971, following the 1964 Niigata and Alaska earthquakes, Seed and Idriss developed the "simplified method," which determines soil liquefaction potential. Seed et al. (1975a, b, 1983, 1985), [16], improved on this strategy. In the early 2000s, more research was conducted to improve this approach, including studies by [6], [7], [10] and [21].

This study examined liquefaction using field data obtained from Turkey and Iraq. [13] estimating the susceptibility of granular materials to probable liquefaction in Basra using SPT data demonstrated that some locations may experience liquefaction of high supposed earthquake magnitude. Other studies have been done to evaluate liquefaction based on SPT in Halbja north of Iraq [2] and Marmora Regine [16].

The possibility of liquefaction is determined by analysing shear wave velocity (V_s), a key dynamic characteristic of soils. V_s values can be calculated using a variety of methods, including traditional geophysical techniques such as seismic refraction and reflection, as well as borehole geophysical methods such as cross-hole and down-hole measurements. To calculate liquefaction potential (PL), parameters such as effective vertical stress ($\sigma'v0$), soil type, and earthquake characteristics are essential. Nevertheless, machine learning plays a vital part in improving liquefaction evaluation processes, thereby reducing both time and costs. It offers an effective set of tools for liquefaction assessments, enabling scientists and engineers to develop accurate, flexible and adaptable models for evaluating liquefaction susceptibility and mitigating seismic risks.

2. Tectonic Features

Turkey, located in the Alpine-Himalayan orogenesis, has a long history of significant quakes across the North Anatolian Fault zone due to its tectonic zones. According to Ketin (1948), the Anatolian-Eurasian plate boundary is characterised by an intracontinental right-lateral strike-slip transform fault that covers approximately 1500 km in northern Turkey. The 1999 Izmit, Duzce, and 1967 Mudurnu earthquakes, which severely devastated the study region and its environs, are the most major earthquakes in the western branch of the NAFZ in the last 60 years. The North Anatolian Fault Zone (NAFZ), which begins with the Karliova triple junction and stretches approximately 1500 km west, is central to this earthquake activity. The Marmara region is a part of the North Anatolian Fault (NAF), which extends towards northern Turkey.

It is situated near the boundary between the Anatolian Plate and the Eurasian Plate, where the plates interact in a challenging manner [16]. The geology of the Marmara region consists of sedimentary, metamorphic, and igneous rocks. The existence of fault zones, such as the North Anatolian Fault and its branches, involves the region's seismic activity. As a result of its proximity to the Sea of Marmara and the presence of soft sediments in coastal areas, the Marmara region is vulnerable to soil liquefaction during earthquakes, which stimulates seismic hazard.

On the other side, Iraq, located southeast of Turkey, shares a border with Turkey's southeastern area. Iraq is located on the northern section of the Arabian Plate and is limited to the north and east by the Bitlis-Zagros Fold and Thrust Belt, which is formed when the Eurasian and Arabian plates collide, causing increased seismic activity. The rest of the country is primarily located on the Arabian Platform, far from major plate borders. The Dead Sea fault system, a large left-lateral transform fault, forms the western boundary of the Arabian Platform, approximately 250 kilometres from Iraq's westernmost point [2]. However, Iraq recently experienced the effects of earthquake epicentres and has the potential for substantial seismic dangers in the future. The northern section of the country is most vulnerable to high-magnitude earthquakes over the next 50 years [1].

3. Methodology

Calculate liquefaction with shear wave velocity depending on soil conditions and the magnitude of the earthquake by measuring three parameters CSR, CRR, and FS. LiquefyPro 5.5 is one of the CivilTech engineering applications established to examine the possibility of liquefaction in seismic conditions. The liquefaction resistance, as measured by seismic testing, was computed using the formula below, The equations below have major factors that are utilised to analyse the potential of liquefaction (PL) in this study. This study identifies LP values based on the categorization of (Appendix 1):

$$FS = \frac{CRR}{CSR} \dots \dots \dots 1$$

$$CRR = \exp \left\{ \frac{[(0.0073.Vs1)^{2.8011} - 2.6168.In(Mw) - 0.0099.1n(\sigma_{v0}) + 0.0028.FC + 0.4809.\Theta^{-1} (PL)]}{1.946} \right\} \dots \dots 2$$

$$Vs1 = Vs \left(\frac{Pa}{\sigma_v} \right)^{0.25} \dots \dots \dots 3$$

$$P_L = \Theta \left(- \frac{0.0073.Vs1^{2.8011} - 1946.In(CSR) - 2.6168(Mw) - 0.0099.In(\sigma_{v0}) + 0.0028.FC}{0.4809} \right) \dots \dots \dots 4$$

Where:

Pa: stress equal to 100 kPa

Vs: shear wave velocity

CRR: cyclic resistance ratio

CSR: cyclic stress ratio

FS: factor safety

PL: probability of liquefaction

In general, Vs values in this study are derived from actual field studies rather than empirical correlations.

The engineering properties of the various strata of many geophysical and soil investigation reports for projects in Iraq, and the parameters are evaluated from field and laboratory test results of the available geophysical and geotechnical investigation reports collected from different sources.

4. Data collection

Data from this study were collected at the regional level. Data from Turkey show two events: Mw: 7.4 1999 Izmit (PGA: 0.41 g), Mw: 7.0 1967 (max: 0.28 g). Mudurnu [16]. Furthermore, various places in Iraq have alternative earthquake scenarios that have been recorded in various locations across Iraqi land [15]. The peak ground acceleration has been estimated using the information in Fig. 1. The key objective of this research is to apply Random Force (RF) to the prediction of liquefaction using Vs measurements.

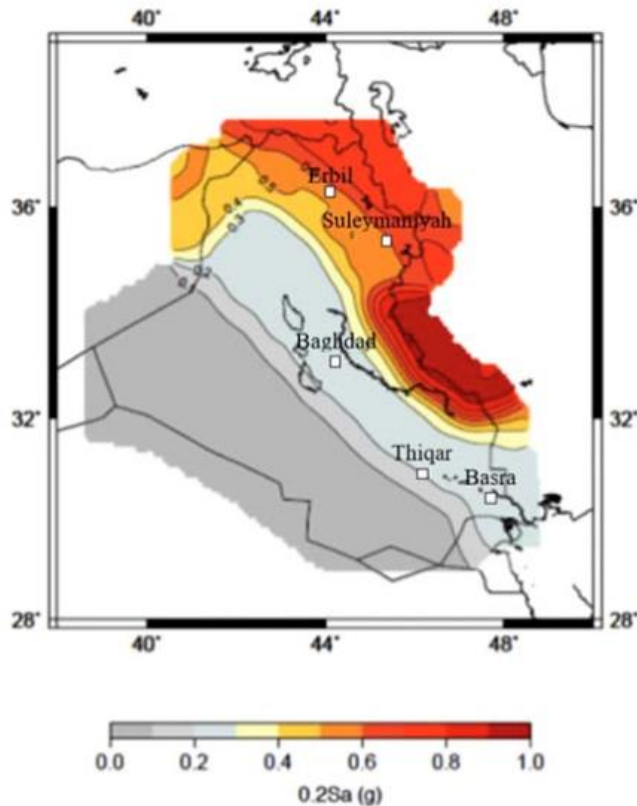


Figure 1 Probabilistic seismic hazard in Iraq with a 2% chance of exceedance in 50 years [1].

5. Random forest (RF)

The Random Forest (RF) methodology is an intelligent recognition system based on statistical learning theory [5]. It uses ensemble learning algorithms to create numerous predictors, making it suitable for both classification and regression problems. Random Forest in this research process as classification which is a method of group learning that improves the accuracy and robustness of classification problems. During training, the algorithm generates a large number of decision trees and outputs the class that represents the mode of the categorization classes. Each decision tree in the random forest is built with a subset of the training data and a random selection of features, which adds diversity to the trees and makes the model more resilient and less prone to overfitting.

Given that liquefaction evaluation often yields two outcomes (liquefaction or non-liquefaction) the study adopts a classification tree approach. The goal is to investigate the correlation between the chance of liquefaction and shear wave velocity. The liquefaction classifier is classified as binary (just 1/-1). [20] to distinguish between two categories, such as liquefaction as 1 and non-liquefaction as -1.

6. Result and Discussion

The input parameters employed include σ'_v , soil type, F_c , V_s , PGA, and M to evaluate the Probability of Liquefaction area of study PL. The data presented in Table (Appendix.1) some areas exhibit no signs of liquefaction, while others demonstrate liquefaction potential. This discovery is reassuring in terms of seismic risk since it suggests that under normal conditions, the soil is less prone to liquefaction-induced damage. However, it is critical to interpret these results with caution, given the differences in liquefaction susceptibility across various locations and soil types.

The research also clearly shows the significance of shear wave velocity (V_s). Higher V_s values often imply firmer soil, which effectively resists liquefaction. Lower V_s values indicate softer, potentially more liquefiable soil. As a result, locations with lower V_s values may be more susceptible to liquefaction, even in the absence of strong seismic activity [14].

Peak ground acceleration (PGA) is an important measure in estimating liquefaction potential since it directly affects the dynamic loading received by the soil during an earthquake. Higher PGA values indicate more ground shaking, which can cause liquefaction in sensitive soils. Thus, even in places with relatively moderate earthquake magnitudes, elevated PGA levels might increase the risk of liquefaction, especially in areas with softer soil [16].

Furthermore, the magnitude of the earthquake (M) significantly influences liquefaction susceptibility. While the overall results show low magnitudes, it is vital to recognise that larger magnitude earthquakes can greatly increase liquefaction potential, particularly in places with susceptible soil conditions [7].

The evaluation of liquefaction by using Random Forest algorithm RF. The general reliability of this model in predicting liquefaction appears to be good. The evaluation matrix shows that accuracy: is 92.22%, precision is 93.5%, Recall: is 93.5%, and specificity is 90.3% with a high precision, which is a proportion of actual liquefaction cases among all predicted cases. Furthermore, the recall and specificity, which represent the percentage of actual liquefaction and non-liquefaction cases, demonstrate effective prediction of liquefaction based on shear wave velocity, given the high performance metric observed.

Table 1 Statistical analysis of the dataset

	M	a max(g)	vs (m/s)	LP
count	219	219	219	219
mean	6.704762	0.347275	247.263004	0.003663
std	0.831688	0.079892	142.041713	1.00183
min	5	0.172	102	-1
25%	6	0.26	181	-1
50%	7.4	0.41	201	1
75%	7.4	0.41	246	1
max	7.5	0.43	1203	1

7. Conclusions

To sum up, our research has yielded significant insights into the evaluation of soil liquefaction potential in Turkey and Iraq through the application of a combination of geotechnical engineering and geophysical studies. It was observed that most of Iraq's regions were less likely to experience liquefaction because of incidents involving low seismic magnitudes and wide divisions from seismic sources; however, some areas were more susceptible because of structural weaknesses in the composition of the soil. This demonstrates how crucial it is to carry out in-depth geotechnical studies in earthquake-prone areas to guarantee the resilience of infrastructure and community safety.

However, Turkey displayed evidence of liquefaction due to its extensive high-magnitude earthquake epicentres, underscoring the necessity of adequate risk mitigation measures. The studies we conducted also revealed the value of

machine learning, specifically the Random Forest algorithm, in predicting liquefaction potential using shear wave velocity. The high accuracy, precision, recall, and specificity seen in our evaluation metrics suggest that this model is reliable in forecasting liquefaction events. These findings emphasise the importance of adding advanced analytical tools into liquefaction assessments to increase prediction precision and catastrophe management.

Acknowledgements

The corresponding author would like to thank Dr. Wisam R. Muttashar for his essential guidance, helpful recommendations, and unwavering support throughout the research process.

References

- [1] Abdalnaby, W., 2019. Structural geology and neotectonics of Iraq, Northwest Zagros. In *Developments in structural geology and tectonics*. Elsevier.
- [2] Al-Taie, E., Al-Ansari, N. and Knutsson, S., 2014. The need to develop a building code for Iraq. *Engineering*, 6(10), pp.610-632.
- [3] Andrus, R.D. and Stokoe, K.H., 1999. Liquefaction resistance based on shear wave velocity.
- [4] Andrus RD, Stokoe KH II (2000) Liquefaction resistance of soils from shear wave velocity. *J Geotech Geoenviron Eng* 126(11):1015–1025.
- [5] Breiman, L. (2001). Random forests. *Machine learning*, 45, 5-32.
- [7] Bhutani, M., & Naval, S. (2020). Assessment of seismic site response and liquefaction potential for some sites using borelog data. *Civ. Eng. J*, 6, 2103-2119.
- [7] Boulanger, R.W. and Idriss, I.M., 2012. Probabilistic standard penetration test–based liquefaction–triggering procedure. *Journal of Geotechnical and Geoenvironmental Engineering*, 138(10), pp.1185-1195.
- [8] Boulanger, R.W. and Idriss, I.M., 2014. CPT and SPT-based liquefaction triggering procedures. Report No. UCD/CGM.-14, 1.
- [9] Castro G (1969) Liquefaction of sands, Harvard Soil Mechanics Series, 81. Pierce Hall, Cambridge,
- [10] Cetin, K.O., Seed, R.B., Der Kiureghian, A., Tokimatsu, K., Harder Jr, L.F., Kayen, R.E. and Moss, R.E., 2004. Standard penetration test-based probabilistic and deterministic assessment of seismic soil liquefaction potential. *Journal of Geotechnical and Geoenvironmental Engineering*, 130(12), p.1314.
- [11] Idriss IM, Boulanger RW (2008) Soil liquefaction during earthquakes. *Earthquake Engineering Research*
- [12] NCEER and 1998 NCEER/NSF workshops on evaluation of liquefaction resistance of soils. *Journal of geotechnical and geoenvironmental engineering*, 1. 2.-3., n.d. NCEER and 1998 NCEER/NSF workshops on evaluation of liquefaction resistance of soils. *Journal of geotechnical and geoenvironmental engineering*, 127(4), 297-313.
- [13] Kennedy, S., & Mahmood, R. A. (2023). Liquefaction Potential Assessment for Basrah Soil Based on Standard Penetration Test Values. *The Iraqi Geological Journal*, 283-293.
- [14] Kayen, R., Moss, R. E. S., Thompson, E. M., Seed, R. B., Cetin, K. O., Kiureghian, A. D., ... & Tokimatsu, K. (2013). Shear-wave velocity–based probabilistic and deterministic assessment of seismic soil liquefaction potential. *Journal of Geotechnical and Geoenvironmental Engineering*, 139(3), 407-419.
- [15] Mohammed, Q. S. A. A. D., & Sa'ur, R. H. (2016). Database for dynamic soil properties of seismic active zones in Iraq. *Journal of Engineering*, 22(7), 1-18.
- [16] Onur, T., Gok, R., Abdalnaby, W., Shakir, A.M., Mahdi, H., Numan, N., Al-Shukri, H., Chlaib, H.K., Ameen, T.H. and Abd, N.A., 2016. Probabilistic seismic hazard assessment for Iraq(No. LLNL-TR-691152). Lawrence Livermore National Lab. (LLNL), Livermore, CA (United States).
- [16] Seed, H. a. I. I., 1971. Simplified procedure for evaluating soil liquefaction potential. Institute, EERI Publication, Monograph MNO-12, Oakland, CA.
- [18] Silahtar, A., Karaaslan, H., & Kocaman, K. (2023). Site Characterization and Liquefaction Hazard Assessment for the Erenler Settlement Area (Sakarya Province, Turkey) Based on Integrated SPT-Vs Data. *Sustainability*, 15(2), 1534.
- [19] Stokoe, K.H., Nazarian II, S., Rix, G.J., Sanchez-Salinero, I., Sheu, J.C., Mok, Y.J., 1988. In situ seismic testing of hard-to-sample soils by surface wave method. In: Von Thun, J.L. (Ed.), *Earthquake Engineering and Soil Dynamics II—Recent Advances in Ground-Motion Evaluation*, 20. Geotech. Spec. Publ., New York, pp. 264–289.

- [20] Watanachaturaporn, P., Varshney, P. K., & Arora, M. K. (2004, May). Evaluation of factors affecting support vector machines for hyperspectral classification. In the American Society for Photogrammetry & Remote Sensing (ASPRS) 2004 Annual Conference, Denver, CO.
- [21] Youd, T.L. and Idriss, I.M., 2001. Liquefaction resistance of soils: Summary report from the 1996 NCEER and 1998 NCEER/NSF workshops on evaluation of liquefaction resistance of soils. Journal of geotechnical and geoenvironmental engineering, 127(4), 297-313.

Appendix 1: Dataset used to calculate LP.

M	a max(g)	vs (m/s)	FC(%)	σ'_v (kPa)	LP (actual)
7.4	0.41	209	4	72	1
7.4	0.41	201	22	85	-1
7.4	0.41	194	47	97	-1
7.4	0.41	170	58	70	-1
7.4	0.41	190	35	124	-1
7.4	0.41	185	35	137	-1
7.4	0.41	162	64	78	-1
7.4	0.41	157	64	142	-1
7.4	0.41	153	65	155	-1
7.4	0.41	207	70	57	1
7.4	0.41	198	61	68	-1
7.4	0.41	191	69	79	-1
7.4	0.41	185	70	90	-1
7.4	0.41	213	68	101	1
7.4	0.41	208	68	112	-1
7.4	0.41	220	70	123	1
7.4	0.41	216	69	134	1
7.4	0.41	206	14	39	-1
7.4	0.41	194	6	49	-1
7.4	0.41	221	6	59	1
7.4	0.41	212	10	70	-1
7.4	0.41	246	16	91	1
7.4	0.41	239	21	101	1
7.4	0.41	233	22	112	1
7.4	0.41	175	26	122	-1
7.4	0.41	172	26	132	-1
7.4	0.41	168	28	143	-1
7.4	0.41	165	24	153	-1
7.4	0.41	242	79	63	1
7.4	0.41	242	65	127	1
7.4	0.41	157	71	60	-1
7.4	0.41	188	76	80	-1
7.4	0.41	151	68	90	-1
7.4	0.41	147	68	100	-1
7.4	0.41	201	70	58	-1
7.4	0.41	195	61	69	-1
7.4	0.41	188	69	81	-1
7.4	0.41	182	70	92	-1
7.4	0.41	190	68	103	-1
7.4	0.41	185	68	114	-1
7.4	0.41	180	70	126	-1
7.4	0.41	189	69	137	-1
7.4	0.41	194	71	65	-1
7.4	0.41	187	68	74	-1
7.4	0.41	204	71	67	-1
7.4	0.41	195	27	79	-1
7.4	0.41	187	63	141	-1
7.4	0.41	183	71	153	-1
7.4	0.41	180	70	165	-1
7.4	0.41	180	30	55	-1
7.4	0.41	211	30	66	-1
7.4	0.41	202	24	78	-1
7.4	0.41	228	32	90	1

7.4	0.41	221	32	101	1
7.4	0.41	215	33	113	1
7.4	0.41	210	32	125	-1
7.4	0.41	205	23	136	-1
7.4	0.41	201	32	148	-1
7.4	0.41	168	85	69	-1
7.4	0.41	161	84	81	-1
7.4	0.41	206	85	73	1
7.4	0.41	198	4	85	-1
7.4	0.41	191	2	98	-1
7.4	0.41	204	3	111	-1
7.4	0.41	198	2	123	-1
7.4	0.41	193	3	136	-1
7.4	0.41	189	2	149	-1
7.4	0.41	160	2	162	-1
7.4	0.41	157	3	174	-1
7.4	0.41	154	3	187	-1
7.4	0.41	189	85	66	-1
7.4	0.41	180	82	80	-1
7.4	0.41	213	84	93	1
7.4	0.41	199	22	121	-1
7.4	0.41	213	88	149	1
7.4	0.41	208	83	162	1
7.4	0.41	124	19	114	-1
7.4	0.41	140	92	73	-1
7.4	0.41	135	92	86	-1
7.4	0.41	199	82	98	1
7.4	0.41	193	88	110	-1
7.4	0.41	188	16	123	-1
7.4	0.41	184	15	135	-1
7.4	0.41	150	15	148	-1
7.4	0.41	147	13	161	-1
7.4	0.41	145	14	174	-1
7.4	0.41	142	13	186	-1
7.4	0.41	137	9.2	46	-1
7.4	0.41	138	8	85	-1
7.4	0.41	236	10	98	1
7.4	0.41	229	15	111	1
7.4	0.41	223	53	124	1
7.4	0.41	217	54	137	1
7.4	0.41	243	83	41	1
7.4	0.41	210	83	52	1
7.4	0.41	200	96	63	-1
7.4	0.41	192	96	74	-1
7.4	0.41	136	96	85	-1
7.4	0.41	132	96	95	-1
7.4	0.41	128	96	106	-1
7.4	0.41	170	34	74	-1
7.4	0.41	213	37	62	1
7.4	0.41	199	40	73	-1
7.4	0.41	211	34	105	-1
7.4	0.41	206	34	116	-1
7.4	0.41	180	51	59	-1
7.4	0.41	171	52	73	-1
7.4	0.41	152	55	99	-1
7.4	0.41	148	70	113	-1
7.4	0.41	195	71	126	-1
7.4	0.41	237	3	69	1
7.4	0.41	227	15	81	1
7.4	0.41	220	13	94	1
7.4	0.41	193	12	106	-1
7.4	0.41	188	9	118	-1
7.4	0.41	176	23	82	-1
7.4	0.41	174	15	117	-1
7.4	0.41	184	27	130	-1
7.4	0.41	179	21	142	-1

7.4	0.41	176	16	155	-1
7.4	0.41	194	93	51	1
7.4	0.41	197	93	64	-1
7.4	0.41	188	93	77	-1
7.4	0.41	181	93	90	-1
7.4	0.41	211	17	103	-1
7.4	0.41	204	16	116	-1
7.4	0.41	199	19	129	-1
7.4	0.41	212	93	142	1
7.4	0.41	207	93	155	1
7.4	0.41	203	93	168	-1
7.4	0.41	199	93	181	-1
7.4	0.41	196	93	194	-1
7.4	0.41	179	28	67	-1
7.4	0.41	197	24	95	-1
7.4	0.41	207	8	135	-1
7.4	0.41	184	43	84	-1
7.5	0.34	173	9	62.1	-1
7.5	0.34	176	11	77	-1
7.5	0.34	181	14	92.3	-1
7.5	0.34	191	13	107.6	-1
7.5	0.34	191	12	122.9	-1
7.5	0.34	194	14	138.8	-1
7.5	0.34	200	15	154.7	-1
6.5	0.23	175	4	62.4	1
6.5	0.23	174	8	77.3	-1
6.5	0.23	179	7	92.5	-1
6.5	0.23	180	4	107.6	-1
6.5	0.23	191	4	122.8	-1
6.5	0.23	193	4	138.7	-1
6.5	0.23	201	5	154.6	-1
7.5	0.3	175	5	140.6	-1
7.5	0.3	196	8	154.4	-1
7.5	0.3	224	12	168.3	-1
7.5	0.3	238	10	182.5	1
7.5	0.3	240	7	196.7	1
7.5	0.3	241	6	210.9	1
6.5	0.24	175	6	141.4	-1
6.5	0.24	192	8	155.3	-1
6.5	0.24	223	11	169.2	-1
6.5	0.24	221	10	183	-1
6.5	0.24	231	7	197.1	-1
6.5	0.24	242	6	211.4	1
6.3	0.4	302	45	35.6	1
6.3	0.4	468	10	109.8	1
6.3	0.4	832	8	58.8	1
6.3	0.4	274	50	52.2	1
6.3	0.4	354	45	121.2	1
6.3	0.4	260	10	28.2	1
6.3	0.4	296	30	74.6	1
6.3	0.4	462	33	159	1
6.1	0.43	262	0	50.2	1
6.1	0.43	576	0	201.7	1
6.1	0.43	384	0	68.8	1
6.1	0.43	233	0	68.8	1
6.3	0.26	219	38	49.4	1
6.3	0.26	301	10	69	1
6.3	0.26	733	10	206	1
6.3	0.26	145	20	29	1
6.3	0.26	212	60	59	1
6.3	0.26	323	60	184.2	1
6.3	0.26	225	18	32.8	1
6.3	0.26	321	60	173.2	1
6.3	0.26	476	0	284.5	1
6.3	0.26	304	66	121.8	1
6.3	0.26	312	65	112.8	1

6.2	0.43	459	66	147.8	1
6.2	0.43	319	22	73.55	1
6.2	0.43	348	5	163.55	1
5.2	0.36	303	10	51	1
5.2	0.36	362	10	76.2	1
5.2	0.36	292	10	26.8	1
5.2	0.36	346	15	57.7	1
6	0.3	606	10	134.3	1
6	0.3	451	6	44.2	1
6	0.3	701	5	117.8	1
6	0.3	186	28	98.8	1
6	0.3	258	9	160	1
6	0.3	265	60	92.2	1
6	0.3	395	30	157.3	1
6	0.3	153	30	98.8	-1
6	0.3	215	25	172.4	1
6	0.3	298	50	108.8	1
6	0.3	428	45	160.8	1
6	0.3	507	10	413.25	1
6	0.3	240	25	110.8	1
6	0.3	430	10	153.8	1
6	0.3	140	20	19	1
6	0.3	219	50	146.12	1
6	0.3	408	10	227.67	1
6	0.3	189	30	69.8	1
6	0.3	248	60	125	1
6	0.3	225	10	271.4	1
6	0.3	165	60	84.8	-1
6	0.3	279	10	126.2	1
6	0.3	260	50	67.1	1
6	0.31	369	10	155.1	1
6	0.31	111	30	22.56	-1
6	0.172	183	20	134.88	1
6	0.172	372	45	122.8	1
6	0.172	398	45	167.3	1
5	0.2	817.8	20	54.3	1
5	0.2	1164	10	117.3	1
5	0.2	1203	5	240.8	1
5	0.2	257	50	62.8	1
5	0.2	379	14	104.8	1
5	0.2	198	50	58.3	1
5	0.2	265	20	92.7	1
5	0.2	497	15	246	1
5	0.2	417	35	186.2	1
5	0.2	312	30	101.15	1
5	0.2	289	0	142.85	1
5	0.2	284	15	50.3	1
5	0.2	550	15	37.7	1
6	0.37	563	18	199.1	1
6	0.37	618	3	86.8	1
6	0.37	268	15	19.1	1
6	0.37	557	5	58.2	1
6	0.37	659	23	148.8	1
6	0.37	111	50	66.2	-1
6	0.37	152	10	151.4	-1
6	0.37	211	50	327.2	1
6	0.37	131	50	50.8	-1
6	0.37	250	50	79.9	1
6	0.37	420	50	268.9	1
5.5	0.2	179	50	98.9	1
5.5	0.2	380	50	198.8	1
5.5	0.2	176	50	53.45	1
5.5	0.2	200	10	53.25	1
5.5	0.2	250	60	145.8	1
5.5	0.2	225	40	58.8	1
5.5	0.2	243	15	69.7	1

5.5	0.2	333	60	205.7	1
5.5	0.2	188	60	25.1	1
5.5	0.2	185	10	30.2	1
5.5	0.2	200	60	136.2	1
5.5	0.2	185	30	84.2	1
5.5	0.2	321	50	121.8	1
5.5	0.25	110	60	126.2	-1
5.5	0.25	145	15	148.2	1
5.5	0.25	166	60	393.2	1
5.5	0.25	200	60	46.88	1
5.5	0.25	240	60	107.66	1
5.5	0.25	329	15	41.3	1
5.5	0.25	627	10	105	1
5.5	0.25	230	3	36.8	1
5.5	0.25	365	15	129.96	1
5.5	0.25	166	50	77.6	1
5.5	0.25	194	10	160.4	1
5.5	0.25	117	50	69.2	-1
5.5	0.25	198	50	135.8	1
5.5	0.25	138	60	95.5	-1
5.5	0.25	103	15	124.99	-1
5.5	0.25	102	50	329.13	-1